Case Studies in Thermal Engineering 24 (2021) 100871

Contents lists available at ScienceDirect

Case Studies in Thermal Engineering

journal homepage: http://www.elsevier.com/locate/csite

An experimental study of a gamma-type MTD stirling engine

Mohammad Hassan Khanjanpour [a], Mohammad Rahnama [b], Akbar A. Javadi [a,*], Mohammad Akrami [a], Ali Reza Tavakolpour-Saleh [c], Masoud Iranmanesh [d]

[a] Department of Engineering, University of Exeter, Exeter, UK
[b] Department of Mechanical Engineering, Shahid Bahonar University of Kerman, Kerman, Iran
[c] Department of Mechanical and Aerospace Engineering, Shiraz University of Technology, Shiraz, Iran
[d] International Center for Science, High Technology and Environmental Sciences, Kerman, Iran

ARTICLE INFO

Keywords:
Stirling engine
γ-type
Swept volume ratio
Finite-dimension thermodynamics
Optimization

ABSTRACT

In this work, a prototype of a γ-type Moderate Temperature Differential (MDT) Stirling engine is manufactured, evaluated, and structurally optimized. An inexpensive mathematical evaluation is carried out based on the finite-dimension thermodynamics (FDT) approach. The optimum swept volume ratio, which contributes to the maximized work and efficiency, is achieved under various conditions based on the temperature difference of 450 K. A computer program is developed to evaluate the performance of the Stirling engine under the assumed working conditions. The swept volume ratio of the engine is found to be 3 for the temperature difference of 450 K. The engine dimensions are then adjusted to fulfil the computed swept volume ratio. The bore and stroke for piston are chosen as 63 mm and 40 mm, respectively. For the displacer, they are selected as 90 mm and 60 mm, respectively, based on the chosen swept volume ratio. Experiments are designed and carried out to verify the output power of the engine at various swept volume ratios, while the device is powered by a Liquefied Petroleum Gas (LPG) heater as simulator of solar energy under atmospheric pressure. The FDT results are shown to be in a very good agreement with the experimental outcomes, whereby the validity of the theoretical approach is confirmed. The findings of this research can be useful as guideline for optimization of MTD Stirling engines.

1. Introduction

Due to the harmful environment effects of using fossil fuels for generating power [1], new ways of electricity generation are needed to be explored that are both clean and efficient. Robert Stirling (a Scottish clergyman) and his brother James (an Engineer) invented the Stirling engine about two centuries ago [2,3] which is theoretically the most efficient (equivalent to the Carnot cycle) device which converts thermal energy to mechanical energy [4]. The development of a solar-powered engine to generate electricity from the sun (as a sustainable source of energy) [5] is very promising for many regions of the world which are facing shortage of electricity, but are rich in terms of solar radiation. An example of such regions is Iran with mean annual solar irradiance of 1800–2200 kWh/m^2 [6]. The Stirling engine is a prominent candidate for power generation which has significant advantages over other similar engines such as external combustion engine. They are commonly found in three different configurations; α, β, and γ. Theses engines are also categorized as High Temperature Differential (HTD) engines, Moderate Temperature Differential (MTD) engines, and Low Temperature Differential (LTD) engines according to the temperature difference considered. The thermal limitation for running of HTD Stirling

* Corresponding author.
E-mail address: A.A.Javadi@exeter.ac.uk (A.A. Javadi).

https://doi.org/10.1016/j.csite.2021.100871
Received 7 October 2019; Received in revised form 10 January 2021; Accepted 29 January 2021
Available online 1 February 2021
2214-157X/© 2021 The Author(s). Published by Elsevier Ltd. This is an open access article under the CC BY license (http://creativecommons.org/licenses/by/4.0/).

Nomenclature

A	Area (m^2)
f	Frequency (Hz)
h	Convective heat transfer coefficient (W/m^2K)
HTD	High Temperature Differential
IP	Indicated-Power (W)
K_a	Thermal conductivity (W/m.K)
k	Dead space volume constant
l	Power piston position (m)
LTD	Low Temperature Differential
M	Torque (N.m)
MTD	Moderate Temperature Differential
m	Mass of working fluid (Kg)
Nu	Nusselt Number
P	Pressure (Pa)
p	Power piston
Pr	Prandtl Number
Q	Heat transfer (J)
R	Gas constant
Re	Reynolds Number
T	Temperature (K)
u	gas velocity (m/s)
V	Volume (m^3)
W	Work (J)
W_t	Total work (J)
y	Displacer position
$\eta(m)$	Efficiency (mechanical)
θ	Phase angle
μ	Gas viscosity (Pa.s)
ξ	Swept volume ratio
ρ	Working fluid density (kg/m3)
σ	Crank angle of power piston (θ-Ω)
τ	Temperature ratio
Ω	Displacer crank angle (^{o})

Subscript

C	Cold outer space
d	Displacer
e	Hot interior space
ed	Hot dead space
H	Hot outer space
i	isothermal
r	Cold interior space
rd	Cold dead space
$\sim$	Reference parameter
$'$	Non-dimensional

engines varies depending on the material utilized to construct it [7]. The efficiency of HTD Stirling engine ranges between 30% and 40% for a temperature range of 923–1073 K, and the typical working speed is within 2000–4000 rpm [8]. However, the cost of electricity produced by HTD engine is around £8000/kW compared to £2500/kW for PV platforms [9]. The thermal efficiency of LTD Stirling engines is less than HTD engines [10], hence their practical application has been limited. Besides the LTD and HTD Stirling engines, the MTD Stirling engines avoid the costly alloys required for HTD and their efficiency is higher than LTD engines. Although the thermal efficiency of moderate temperature differential (MTD) Stirling engines is higher than low temperature differential (LTD) engines, the complexity of design of MTD engines has led to the lack of research in this field.

Due to the above mentioned advantages, recently there has been some interest to develop MTD Stirling engines. Karabulut et al. [11] introduced the first practical MTD model for the Stirling engine in 2000. They constructed and tested an α-type Stirling engine in temperature range of 873° – 1373 K and pressure between 1 and 4 bar. The maximum output power of 65 W was obtained at 1373 K and 2.5 bar pressure. This indicates that increasing the pressure inside the Stirling engine does not always increase the output power, hence

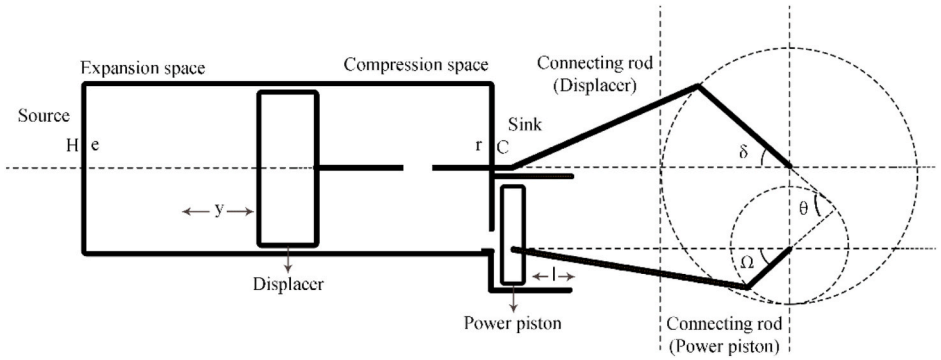

Fig. 1. Initial design of γ-type MTD Stirling engine.

the optimum pressure should be determined for the engine. In 2005, Cinar et al. [12] constructed and examined a β-type Stirling engine with a total swept volume of 192 cc under atmospheric pressure. The performance of the engine was studied using an electric heater at temperatures 1073, 1173, and 1273 K. At temperature of 1273 K and rotational speed of 208 rpm, the test engine reached an output power of 5.98 W. The results indicate that despite the high temperature of the hot source, a high output power cannot be achieved from Stirling engines at atmospheric pressure. A test MTD Stirling engine was studied by Sripakagorn and Srikam [13] who reported that at 205 rpm, the maximum power outputs were 3.8 W at 623 K and under atmospheric pressure and 95.4 W at 723 K and 7 bar. Their research showed that MTD Stirling engine could provide a performance equivalent to HTD engine with simpler and less expensive development. In 2015, Gheith et al. [14], investigated different regenerators for an γ-type MTD Stirling engine and showed that a stainless steel regenerator with a porosity of 85%, under temperature of 773 K and pressure of 8 bar achieved the highest efficiency of 26%. Recently, Lai et al. [15] carried out a theoretical study to investigate the potential use of MTD Stirling engine for a desalination system. They found that efficiency of MTD Stirling engine increases linearly with increasing the temperature of the heater. The theoretical conversion rate (thermal to mechanical energy) changed from of 30.5%–44.5% when temperature increased for 573 K–773 K.

A review of the literature shows that there has been no detailed research on swept volume ratio, which plays an important role in the mechanical performance of the MTD Stirling engines. The main goal of this research is to develop, validate and use an inexpensive method to optimize a γ-type MTD Stirling engine in order to maximize its mechanical performance. According to the desired temperature difference and using the finite-dimension thermodynamics approach, the optimum swept volume ratio of the engine is estimated in order to maximize the objective functions (e.g. efficiency and work). Based on the obtained swept volume ratio, a prototype of the MTD Stirling engine is designed, manufactured and evaluated. The manufactured engine is evaluated experimentally to demonstrate the potential of the MTD Stirling engine. The performance of the engine is compared with the results published in the literature.

The findings of this research have improved the current understanding of the behavior of MTD Stirling engine, both experimentally and numerically, and highlighted the importance of main design parameters. The results showed that the finite dimension thermodynamics method is an effective tool for optimization of MTD Stirling engine by using only few experiments. It was also shown that there is an important relationship between the swept volume ratio and thermal performance of the MTD Stirling engine.

2. Optimization process

Determining the optimum swept volume ratio (ξ) (the ratio of the swept volume of the power piston to the swept volume of displacer piston) is the most important objective in the design and optimization of a Stirling engine. Accordingly, in the current study, the design parameter for optimization is swept volume ratio (ξ) and the objective functions are non-dimensional work (w') as well as efficiency (η). The Finite-Dimension Thermodynamics (FDT) method [16] and the geometry of the γ-type Stirling engine are used to determine the relationship between the non-dimensional work (w') and efficiency (η) in order to find the optimum swept volume ratio (ξ) [17].

To solve the complex equations of the FDT method and obtain meaningful results, some simplifying assumptions are necessary.

In this study, seven assumptions are considered for simplifying the mathematical equations as fellows:

(1) The working fluid is an ideal gas; (2) The engine does not have gas leakage and the mass of the gas stays unchanged; (3) There is no regeneration; (4) Compression and expansion processes are isothermal; (5) The dead volume of each zone is assumed a constant ratio of the volume; (6) The heat can only be transferred via the displacer cylinder wall; and (7) The expansion and constriction spaces have sinusoidal movement.

Fig. 1 illustrates the initial design of the MTD Stirling engine with γ-configuration (without regenerator) which will be developed mathematically and optimized in this section.

The calculation procedure for identifying the optimal swept volume ratio can be summarized into six steps. The flowchart of the whole process is shown in Fig. 2.

According to thermodynamics laws, the work (W) and efficiency (η) of a closed system can be determined using equations (1) and

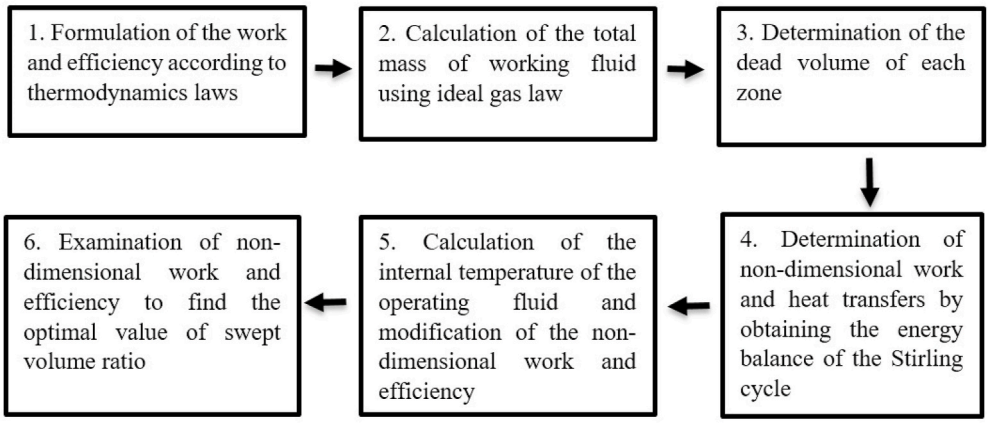

Fig. 2. The flowchart of the procedure for identification of the optimal swept volume ratio.

(2), respectively [18].

$$W = -\oint P dl \tag{1}$$

$$\eta = \frac{W}{Q_e} \tag{2}$$

where P: the pressure of working fluid; l: the power piston position; Q_e: the expansion heat transfer.

The ideal gas law (Eq. (3)) can be utilized to determine the pressure of the working fluid (Assumption 1) [19].

$$PV = mRT \tag{3}$$

where V: the volume of working fluid; m: the mass of working fluid; T: the temperature of working fluid; R: the gas constant.

The total mass of working fluid in a Stirling engine (in the hot and cold spaces together) can be expressed by the sum of total masses contained in the engine by considering Assumptions 2, 3 & 4 as follows [20]:

$$m = \sum m_i = m_r + m_e = \frac{P(V_r + V_{rd})}{RT_r} + \frac{P(V_e + V_{ed})}{RT_e} \tag{4}$$

where V_{rd}: the compression space dead volume; r: the compression space; V_{ed}: the expansion space dead volume; e: the expansion space.

The total dead volume is defined as the sum of the void volumes of Stirling engine and these volumes are considered for regenerator and cold and hot cylinders [21]. In normal Stirling engine design practice, the total dead volume is about 58% of the total volume [22]. In the current research, the dead volume of each zone is assumed a constant ratio of the volume (Assumption 5) as follows:

$$V_{rd} = k(V_r) \tag{5}$$

$$V_{ed} = k(V_e) \tag{6}$$

Consequently:

$$m = \frac{(l+k)P}{RT_r}\left[xA_p + (y_0 - y)A_d\right] + \frac{(l+k)P}{RT_e}\left[yA_d\right] \tag{7}$$

where k: the dead volume constant; A_p: the area of power piston; A_d: the area of displacer piston; y: the displacer's stroke; l: the power piston's stroke; y_0: the difference between the length of displacer cylinder and displacer piston.

To find the relationship between work (W) and efficiency (η), a dimensionless mass parameter (m') is defined as follows [23]:

$$m^{\sim} = \frac{P^{\sim} V_p}{RT_r} \tag{8}$$

$$\xi = \left(\frac{V_d}{V_p}\right) = \frac{A_d y_0}{A_p l_0} \tag{9}$$

$$m' = \frac{m}{m^{\sim}} = (1+k)P'\left([l' + (1-y')\xi] + \frac{1}{\tau}[y'\xi]\right) \tag{10}$$

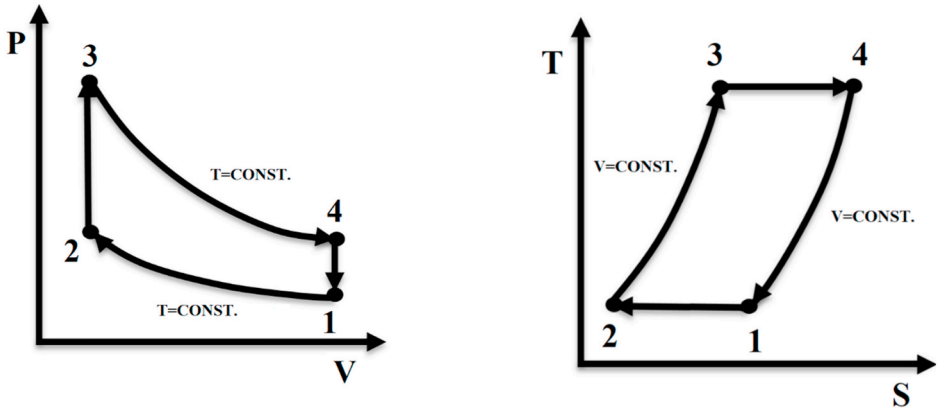

Fig. 3. *P–V* (a) and *T-S* (b) diagrams of Stirling engine.

where ξ: the swept volume ratio; $m^{\sim}$: the reference mass; $P^{\sim}$: the reference pressure; V_d: displacer swept volume; P': the dimensionless pressure; V_p: the power swept volume.

Eq. (10) can be rearranged as:

$$P' = \frac{m'}{(1+k)\left([l' + (1-y')\xi] + \frac{1}{\tau}[y'\xi]\right)} \tag{11}$$

Accordingly, the dimensionless work (W')is expressed as [16]:

$$W' = -\oint P' dl' \tag{12}$$

Fig. 3 shows the P–V and T-S diagrams for an ideal Stirling cycle with four processes, including isothermal contraction (1–2), isochoric heat absorption (2–3), isothermal expansion (3–4), and isochoric heat exclusion (4–1) [24,25].

By obtaining the energy balance of the Stirling cycle, non-dimensional work (W') and transfer heats are calculated as [17]:

$$\tau = \left(\frac{T_e}{T_r}\right) \tag{13}$$

$$V_e = yA_d + V_{hd} \tag{14}$$

$$V_r = lA_p + (y_0 - y)A_p + V_{rd} \tag{15}$$

$$W' = -\oint P' dl' = -\left[\int_1^2 P'(l',0)dl' + \int_3^4 P'(l',1)dl'\right] = \frac{-m'}{(1+k)}\left[\int_1^0 \frac{dl'}{(l'+\xi)} + \int_0^1 \frac{dl'}{l'+\frac{\tau}{\xi}}\right] = \frac{-m'}{(1+k)}\ln\left(\frac{\tau+\xi}{\xi+1}\right) \tag{16}$$

$$Q_e^{i} = \frac{1}{P^{\sim}V_p}\oint P dV_e = \xi\oint P' dV_e = \frac{m'}{1-\tau}\ln\left(\frac{1}{\tau}\right) \tag{17}$$

$$Q_r^{'i} = \frac{1}{P^{\sim}V_p}\oint P dV_r = \oint P'(dl' - \xi dy') = \frac{-m'}{1-\tau}\ln\left(\frac{1}{\tau}\right) \tag{18}$$

where τ: the temperature ratio; (): the non-dimensional parameters; i: the isothermal process.

Finally, the engine efficiency (η) which only depends on dead volume ratio (k) and temperature ratio (τ) can be determined by dividing work over transferred heat to the Stirling engine [26,27]:

$$\eta = \frac{|W'|}{Q_e^{i}} = \frac{\frac{-m'}{(1+k)}\ln\left(\frac{\tau+\xi}{\xi+1}\right)}{\frac{m'}{1-\tau}Ln\left(\frac{1}{\tau}\right)} = \frac{1-\tau}{1+k}\ln\left(\frac{\tau(\tau+\xi)}{\xi+1}\right) \tag{19}$$

It is important to note that in the design of Stirling engine, the temperature of the internal operating fluid at the expansion space is always lower than that of the hot source, and also in the contraction space, the air temperature is higher than the cold sink [28].

Table 1
Initial parameters of the Stirling engine.

$T_H(K)$	$T_C(K)$	$P_1(KPa)$	k	$f\ (rev\ s^{-1})$	$y_0(cm)$
753	303	101	0.15	2	6

Therefore, the convective heat transfer equations are used to obtain the relationship between the internal and source temperatures as follows [17]:

$$Q_e = \frac{h_e A_d}{f}(T_H - T_e) = \frac{h_e A_d}{f}\ T_H\left(1 - \frac{T_e}{T_H}\right) \tag{20}$$

To make Q_e non-dimensional, it is divided by P_1 and V_p as:

$$\acute{Q_e} = \frac{Q_e}{P^{\sim} V_p} = \frac{h_e A_d}{f P^{\sim} y_0}\ (T_H - T_e) \tag{21}$$

where h_e: the expansion convective heat transfer coefficient; f: the frequency; T_H: the temperature of hot source.

Consequently, T_e can be determined from Eqs. (18) and (21):

$$T_e = T_H - \frac{-\acute{m} P^{\sim} y_0 \tau}{h A_d (1-\tau)} \ln\left(\frac{1}{\tau}\right) \tag{22}$$

The temperature of the compression (T_r) can be determined following the same procedure [17]:

$$Q_r = \frac{h_r A_d}{f}(T_C - T_r) = \frac{h_r A_d}{f}\ T_C\left(1 - \frac{T_r}{T_C}\right) \tag{23}$$

$$\acute{Q_r} = \frac{Q_r}{P^{\sim} V_p} = \frac{h_r A_d T_H}{f P^{\sim} V_p \tau}\ \left(1 - \frac{T_r}{T_C}\right) \tag{24}$$

where h_r: the compression convective heat transfer coefficient; T_r: the temperature of cold source.

T_r can also be determined from Eqs. (23) and (24):

$$T_r = T_C - \frac{f P^{\sim} V_p \acute{m}}{h A_d (1-\tau)} \ln\left(\frac{1}{\tau}\right) \tag{25}$$

In order to estimate the convective heat transfer coefficient in both sides (h_e and h_r), the Dittus–Boelter equation (Eq. (27)) for heat transfer in turbulent and oscillating flow and in smooth circular pipes can be used [29]. This is one of the formulas which was used for estimating heat transfer coefficient in Stirling engines in previous research works [30–32]. In this equation, it is assumed that the heat transfer is in the displacer cylinder and that heat can be transferred only through the wall of displacer cylinder which can be assumed as a circular tube (assumption 6). It should be emphasized here that this assumption may result in some error, however it is an appropriate way to find the approximate heat convection coefficients for Stirling engines. Moreover, since in design of any type of engine, the initial parameters are necessary [33–36], the rotational speed of engine (ω) was assumed as 2 rev/s (Table 1), and the gas velocity (u) which is produced by movement of displacer was calculated based on the rotational velocity. The convective heat transfer coefficients are calculated as follows:

$$Nu = (0.23) Re^{0.8} Pr^{G} \tag{26}$$

$$Re = \frac{hD}{K_a} \tag{27}$$

where Nu: the Nusselt number; Re: the Reynolds number; Pr: the Prandtl number; $G = 0.4$ for heating; $G = 0.3$ for cooling; h: the heat transfer coefficient; K_a: the thermal conductivity of working fluid; ρ: the gas density of working fluid; u: the gas velocity; μ: the gas viscosity; D: the diameter of flow section (displacer cylinder).

Using Eqs. (26) and (27) as well as the thermodynamics table for air properties (with $T_e = 303$ K, $T_r = 753$ K) [37], the values of heat transfer coefficient of both sides (h_r and h_e) are calculated as: $h_e = 17.67$ W/(m^2.K), and $h_r = 28.72$ W/(m^2.K).

Lastly, the internal expansion and contraction space temperatures are calculated using a computer program coded in MATLAB, and the respective values of T_e and T_r are 612.3 K and 423.5 K. As mentioned before, for designing and manufacturing a Stirling engine, considering initial parameters is essential. The initial parameters of the considered MTD Stirling engine are summarized in Table 1. The determined objective functions, i.e., non-dimensional work (Eq. (16)) and efficiency (Eq. (19)), are examined in order to find the optimal value of swept volume ratio. This is done using a program developed in MATLAB and the results are plotted in Fig. 4. Similar patterns of non-dimensional work and swept volume ratio are reported in Cheng et al. [38]. As it can be seen in Fig. 4, ξ is determined as 3 (average of 3.1 and 2.9) to maximize both the work and efficiency.

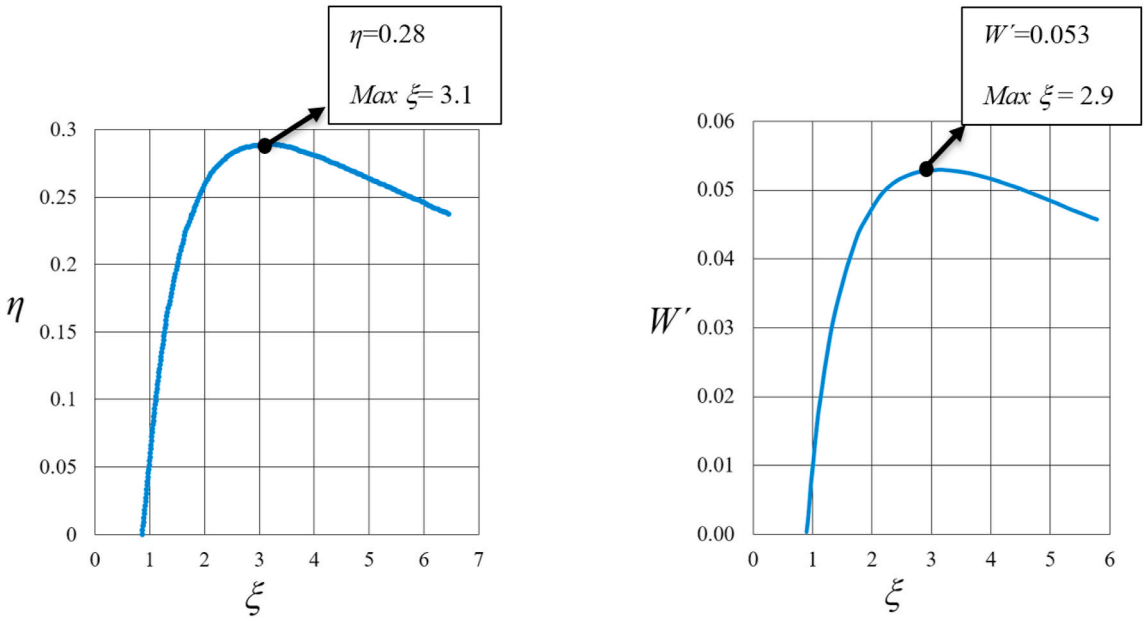

Fig. 4. Variations of the Stirling engine's efficiency (η) (left) and dimensionless work (W') (right) versus swept volume ratio (ξ).

Table 2
Key parameters of the engine design.

Type of engine	Displacer	Power piston	Phase angle	Swept volume ratio	Working gas	Cooling system
Gamma	Bore × Stroke: 9 × 6 (cm)	Bore × Stroke: 6 × 4(cm)	90°	3	Air	Air cooled

3. Engine construction

Based on the results obtained in the previous section, a moderate differential temperature Stirling engine with γ-configuration is developed. Table 2 shows the key parameters of the engine design. The power cylinder and power piston are made of a cast iron pipe and aluminum, respectively. The power piston turns to match the bores of the power cylinder. The clearance between the power piston and cylinder is 0.02 mm according to recommendations from previous research. The displacer and the displacer cylinder are built from aluminum and steel pipe respectively. The displacer piston and the displacer cylinder have a clearance space of 1.0 mm which was also used by Cinar and Karabulut [39]. The rod of the displacer is made of stainless steel. Moreover, the cooling fins are built from aluminum. The two middle pages are made of aluminum with dimensions 20 × 16 × 2 (cm) and are connected by 14 bolts and nuts. Finally, the flywheel is constructed from iron with 20 cm thickness and 2.3 kg weight, based on the guidelines presented by Shiferaw et al. [40]. Photographic images of the γ-type Stirling engine developed in this work are shown in Fig. 5 (a) & (b).

4. Experimental study

4.1. Measurement apparatus

An experimental system is designed and set up [Fig. 5 (c)] for the evaluation of output of the constructed MTD Stirling engine. A thermocouple is used to measure the temperature of the cooler (sink), T_C, while the temperature of the heater (source), T_H, is measured by the laser thermometer. A data logger (ST-8891E) and a laptop are utilized to collect data from the thermocouple and laser thermometer. The temperature is measured with accuracy of 1 K. Moreover, the torque (M) of the engine is measured by an electrodynamometer with the moment's rage of 0–2 Nm with an accuracy of 0.001 Nm. The variations in voltage of the electrodynamometer are applied by an AC power supply. The engine speed (n) is measured using a digital tachometer, RM-1501, with measuring range of 0–99.990 rpm and accuracy of 0.1 rpm. A domestic gas burner is used to power the engine. It is supplied with a Liquefied Petroleum Gas (LPG) tank, and has an adjustable nozzle and a pressure regulator. The accuracy of measurement for the gas mass is ± 0.01 kg.

An uncertainty analysis of the tested parameters is performed according to Refs. [41,42]. The uncertainty of each factor is measured with a reliability of 96% and the results are shown in Table 3.

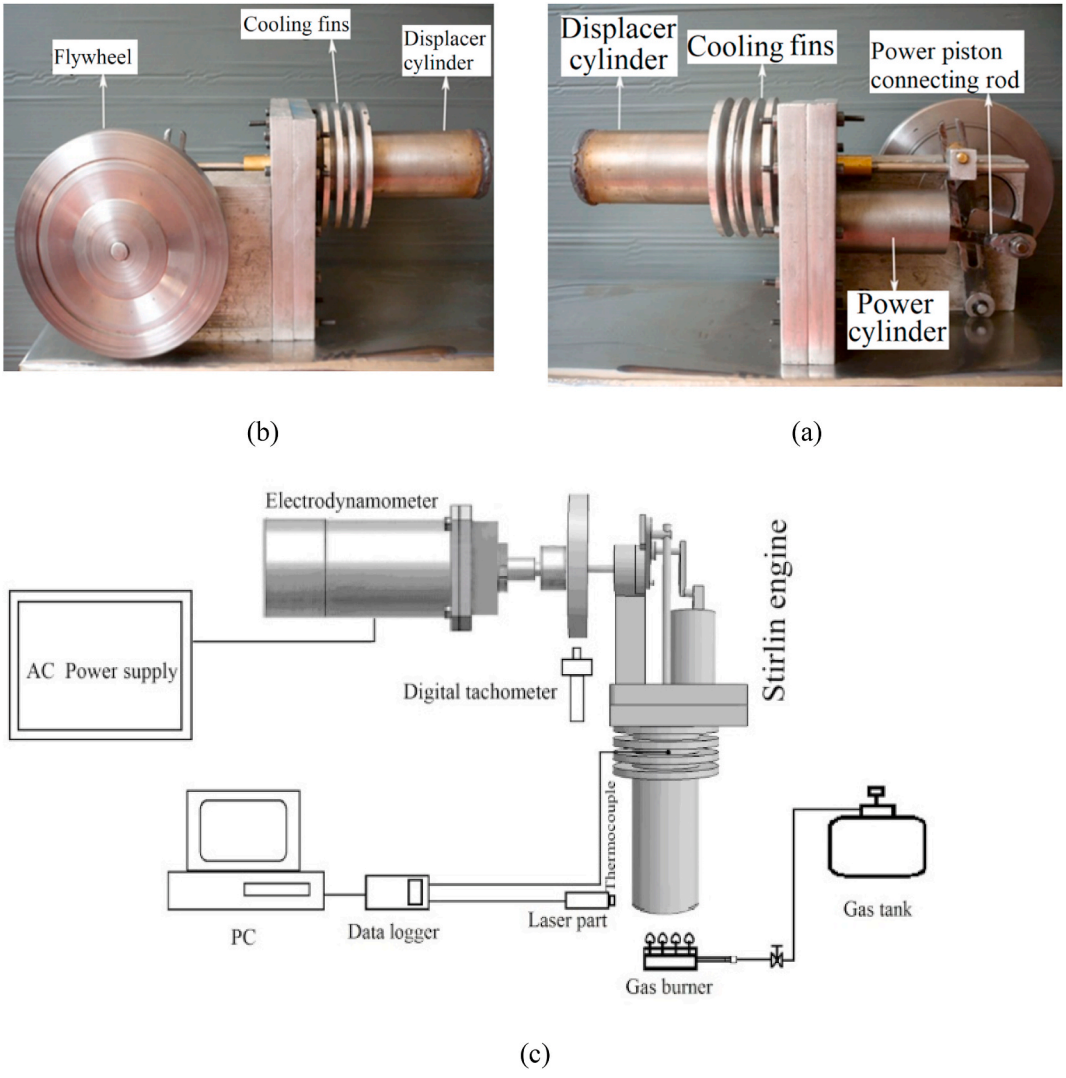

Fig. 5. (a) Rear and (b) front views of the constructed γ-type MTD Stirling engine, and (c) measurement system for the Stirling engine.

Table 3
Uncertainties of tested parameters.

Tested parameters	Normal value	Uncertainty	Relative uncertainty
T_H	473–873 K	1 K	0.14%
T_C	293–308 K	1 K	0.33%
M	0.01–0.18 Nm	0.001 Nm	1.05%
N	100–220 rpm	0.1 rpm	0.06%

4.2. Indicated-power

The mean indicated-power (*IP*) of an MTD Stirling engine can be calculated as [43]:

$$IP = \frac{W_t\, n_{mean}}{60} \tag{28}$$

where W_t is the total amount of work of engine and n_{mean} is the mean engine speed. To calculate the W_t, the Schmidt theory can be used [44,45]. The Schmidt model is focused on the isothermal expansion and compression of an ideal gas [46]. Although, it applies the ideal Stirling cycle, the theory has had acceptable results in Stirling engine design thus far [47,48]. Assuming simple variation of the harmonic volume enables to determinate pressure as a function of the angle of the crank and contributes to work cycle. The Schmidt

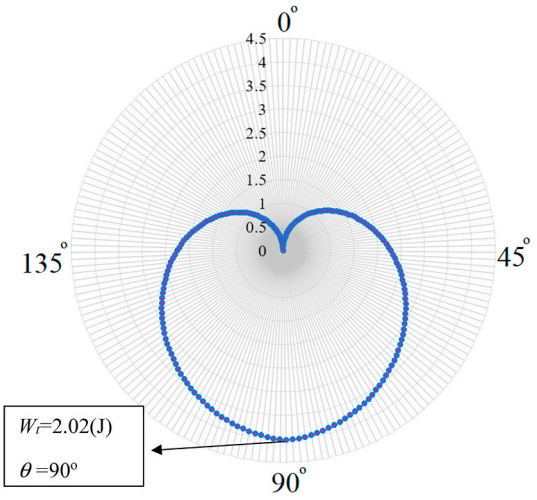

Fig. 6. Variations of W_t with different phase angles (θ °).

theory has been presented in different forms based on the engine types utilized and can be exploited for Stirling engines γ-configuration [49]. As the temperatures of the internal compression space were measured before (see Section 2) considering the proposed model, the Schmidt theory with all of its related assumptions is used to evaluate the total work (W_t) of the engine and the optimum angle of the phase (θ). Based on the mechanical configuration shown in Fig. 1, and by considering Assumption 7, the momental expansion and contraction volumes are as follows [50]:

$$V_e = V_{ed} + \frac{V_d}{2}(1-\cos(\Omega)) = V_d\left(k + \frac{1}{2}(1-\cos(\Omega))\right) \tag{29}$$

$$V_r = V_{rd} + \frac{V_p}{2}(1-\cos(\Omega-\theta)) + \frac{V_p}{2}\left(1+(1+\cos(\Omega))V_r = V_p\left(k+\frac{1}{2}\left(1-\cos(\Omega-\theta)\right)\right) + \frac{V_d}{2}(1+\cos(\Omega))\right. \tag{30}$$

where Ω: the displacer crank angle; θ: the phase angle.

By considering Assumptions 2, 3 & 4 and using the ideal gas law [16]:

$$m = \frac{P}{R}\left[\frac{V_r}{T_r} + \frac{V_e}{T_e}\right] = \frac{P}{T_r R}\left[V_r + \frac{V_e}{\tau}\right] = \frac{PV_d}{RT_r}\left[\left(k + \frac{1}{2}(1-\cos(\Omega))\right) + \frac{1}{\tau\xi}\left(k + \frac{1}{2}(1-\cos(\Omega-\theta))\right) + \frac{1}{2\tau}(1+\cos(\Omega))\right] \tag{31}$$

$$P = \frac{mRT_r}{V_d\left[\left(k+\frac{1}{2}(1-\cos(\Omega))\right) + \frac{1}{\tau\xi}\left(k+\frac{1}{2}(1-\cos(\Omega-\theta))\right) + \frac{1}{2\tau}(1+\cos(\Omega))\right]} \tag{32}$$

The works on both sides can be determined by substituting the pressure equation as follows [16]:

$$W_e = -\oint PdV_e = \frac{mRT_r}{2}\int_0^{2\pi} \frac{\sin(\Omega)}{\left(k+\frac{1}{2}(1-\cos(\Omega))\right) + \frac{1}{\tau\xi}\left(k+\frac{1}{2}(1-\cos(\Omega-\theta))\right) + \frac{1}{2\tau}(1+\cos(\Omega))} d\Omega \tag{33}$$

$$W_r = -\oint PdV_r = \frac{mRT_c}{2\xi}\int_0^{2\pi} \frac{\sin(\Omega-\theta)}{\left(k+\frac{1}{2}(1-\cos(\Omega))\right) + \frac{1}{\tau\xi}\left(k+\frac{1}{2}(1-\cos(\Omega-\theta))\right) + \frac{1}{2\tau}(1+\cos(\Omega))} d\Omega$$

$$\frac{mRT_r}{2}\int_0^{2\pi} \frac{\sin(\Omega)}{\left(k+\frac{1}{2}(1-\cos(\Omega))\right) + \frac{1}{\tau\xi}\left(k+\frac{1}{2}(1-\cos(\Omega-\theta))\right) + \frac{1}{2\tau}(1+\cos(\Omega))} d\Omega \tag{34}$$

And finally, the total work (W_t) of engine per each cycle can be defined as follows [16]:

$$W_t = W_e + W_r = \frac{mT_r}{2\xi}\int_0^{2\pi} \frac{\sin(\Omega-\theta)}{\left(k+\frac{1}{2}(1-\cos(\Omega))\right) + \frac{1}{\tau\xi}\left(k+\frac{1}{2}(1-\cos(\Omega-\theta))\right) + \frac{1}{2\tau}(1+\cos(\Omega))} d\Omega \tag{35}$$

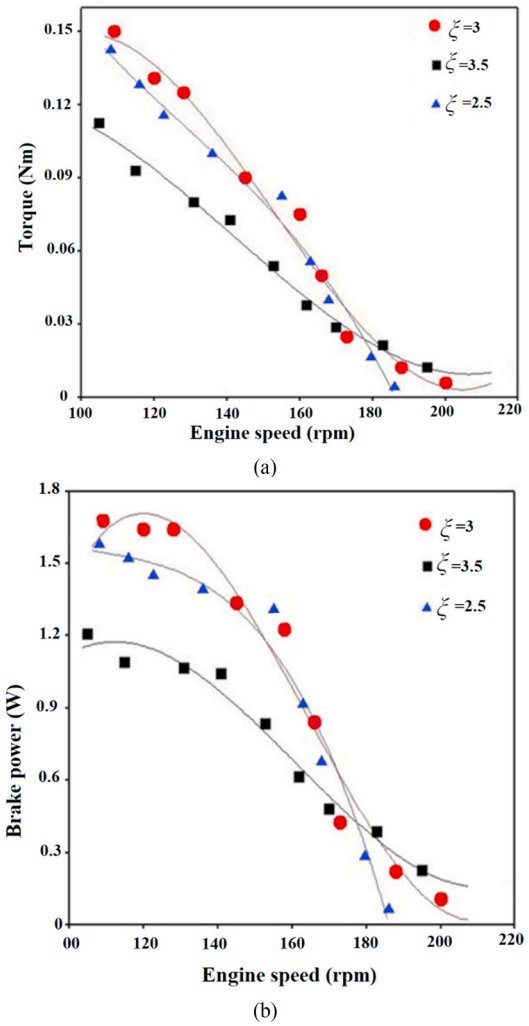

Fig. 7. Variations of (a) engine speed VS engine torque and (b) engine speed VS brake power.

Considering the outcome of the optimization model and the data in Table 1, it is possible to evaluate W_t and the optimal phase angle. Eq. (35) is analyzed using a computer program developed in MATLAB and the results are plotted as the variation of W_t per single cycle as a function of phase angle to calculate the optimum phase angle and the maximum W_t (Fig. 6). W_t is found to be maximum at phase angle (θ) of 90°. The theoretical value of W_t is found as 2.02 (J) without any process of regeneration. In the end, by substituting the obtained W_t and n_{mean} into Eq. (28), the indicated-power is calculated as 5.28 W. This value is reasonable based on the fact that in a non-pressurized Stirling engine without regenerator which operates at atmospheric pressure, the output power is in the range of a few watts [51–53]. Obviously, by increasing the internal pressure of the engine (e.g. helium or hydrogen) [54] and using a regenerator [55], a very high power can be achieved with this engine. It is worth noting that the total amount of operating fluid (total inside volume of engine multiplied by density) is only about 1.0 g.

4.3. Experimental tests

The developed MTD Stirling engine is tested in the Thermodynamics Laboratory in order to assess the validity of the obtained swept volume ratio from the optimization study. Based on the presented optimization technique, the optimum swept volume ratio is found to be 3. Thus, the experimental investigation is organized with three swept volume ratios 2.5, 3 and 3.5 so as to see whether or not the swept volume ratio of 3 is optimal. To achieve three different swept volume ratios, 3 different power pistons (with different diameters) and 3 different power cylinders are used, all on the same engine.

The brake power of the engine is calculated as follows [28]:

$$P_{Brake=\frac{2\pi Mn}{60}} \tag{36}$$

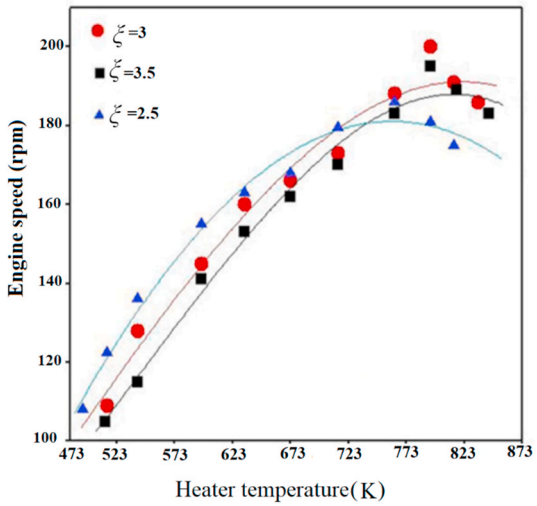

Fig. 8. Variations of heater temperature with engine speed.

where n: the engine's rotational speed (rpm); M: the engine torque (Nm).

Fig. 7 shows the variations of the torque and the brake power of the Stirling engine with the engine speed for the three swept volume ratios. The results show that a higher engine torque and a higher brake power can be achieved at lower engine speeds. A similar pattern for the output power of γ-type Stirling engine versus the engine speed has been reported by Kang et al. [39]. Furthermore, around the engine speed of 120 rpm, which is the considered speed in the optimization study (see Table 1), the swept volume ratio of 3 showed some improvement in compared with other graphs which confirms the validity of the optimization analysis.

The indicated power of the presented MTD Stirling engine is found as 5.36 W at 160 rpm. Experimentally it is found that the brake power is 1.31 W at the mentioned speed (see Fig. 7). The difference can be attributed to the absence of regeneration as well as thermal and mechanical losses. Accordingly, the mechanical efficiency (η_m) as the ratio of indicated power over brake power [56] is 24%.

Fig. 8 shows the variations of the speed of the engine with the heater temperature for the three swept volume ratios. The results show that the engine's speed is increased sharply with increasing the heater temperature. Around the assumed heater temperature of 507 K (see Table 1), the maximum engine speed can be observed for the swept volume ratio of 3 which is further evidence to show the validity of the optimization scheme.

According to Fig. 8, the maximum engine speeds for swept volume ratios of $\xi = 2.5$, $\xi = 3.0$ and $\xi = 3.5$ are 180, 198 and 190 rpm (at different temperatures), respectively. It can be seen that the engine speed with swept volume ratio $\xi = 3.0$ is higher than $\xi = 2.5$ and $\xi = 3.5$. In Stirling engines, the engine speed increases with increasing temperature up to a certain point (due to heat loss) beyond which, further increase in temperature will decrease the engine speed. The purpose of this comparison was to find an appropriate swept volume ratio which can transfer the heat better. It is shown that the swept volume ratio of $\xi = 3.0$ can provide a higher speed than the other tested engines at different temperatures.

5. Conclusions

In the present study, a γ-type moderate temperature differential Stirling engine (non-pressurized) with adjustable swept volume ratio was developed and manufactured to optimize the swept volume ratio in order to maximize the mechanical performance. To evaluate the lowest output capacity and to simplify the Stirling engine structure, the regenerator was ignored. To validate the obtained optimum swept volume ratio, the engine was experimentally evaluated at different swept volume ratios. The main conclusions are as follows:

1) Application of the finite dimension thermodynamics approach has made it possible to obtain meaningful results for inexpensive optimization of the MTD Stirling engine.
2) The combination of the swept volume ratio of 3 and phase angle of 90° leads to maximum engine efficiency and maximum non-dimensional work for the temperature difference between hot and cold source of 450 K.
3) The thermal and mechanical efficiencies of the presented MTD Stirling engine are calculated as 28% and 24.4% respectively.
4) The indicated power of the Stirling engine is measured as 5.36 W at 160 rpm. However, experimentally it is found that the brake power is 1.31 W at the same speed. The difference can be attributed to the absence of regeneration as well as thermal (irreversibility) and mechanical losses.
5) The development and analytical methods described in this article have been validated by experimental tests which can be used by investigators and designers for future production of the MTD Stirling engines.

Author statement

Khanjanpour M.H., **Rahnama M.**, **Javadi A.A.**, and **Tavakolpour-Saleh A.R.**: Conceptualization, Methodology and Model development; **Khanjanpour M.H.**: Experimental testing, Writing, Original draft preparation, and Visualization; **Rahnama M.** and **Javadi A.A.**: Supervision; **Khanjanpour M.H.**, **Javadi A.A.**, and **Akrami M.**: Validation; **Javadi A.A.**, **Iranmanesh M.**, and **Akrami M.**: Reviewing and Editing.

Declaration of competing interest

The authors declare that they have no known competing financial interests or personal relationships that could have appeared to influence the work reported in this paper.

Acknowledgement

The authors would like to acknowledge the financial support from the Department of Mechanical Engineering of the Shahid Bahonar University of Kerman as well as Kerman Graduate University of Technology.

References

[1] W.S. Ebhota, T.-C. Jen, Fossil fuels environmental challenges and the role of solar photovoltaic technology advances in fast tracking hybrid renewable Energy System, International Journal of Precision Engineering and Manufacturing-Green Technology 7 (1) (2020) 97–117.
[2] G. Walker, Stirling Engines, 1980.
[3] C. Maier, et al., Stirling Engine, University of Gavle, 2007.
[4] D.A. Renfroe, A COMPUTER MODEL OF A STIRLING ENGINE USING A TWO-PHASE TWO-COMPONENT WORKING FLUID, 1982.
[5] M.d.A. Al-Nimr, W.A. Al-Ammari, A novel hybrid and interactive solar system consists of Stirling engine/vacuum evaporator/thermoelectric cooler for electricity generation and water distillation, Renew. Energy 153 (2020) 1053–1066.
[6] R. Panahi, et al., Analysis of the thermal efficiency of a compound parabolic Integrated Collector Storage solar water heater in Kerman, Iran, Sustainable Energy Technologies and Assessments 36 (2019) 100564.
[7] I. Tlili, Y. Timoumi, S.B. Nasrallah, Analysis and design consideration of mean temperature differential Stirling engine for solar application, Renew. Energy 33 (8) (2008) 1911–1921.
[8] A. Asnaghi, et al., Thermodynamics performance analysis of solar stirling engines, ISRN Renewable Energy 2012 (2012).
[9] D. Mills, Advances in solar thermal electricity technology, Sol. Energy 76 (1–3) (2004) 19–31.
[10] S. Isshiki, et al., The experimental study of atmospheric Stirling engines using pin-fin arrays' heat exchangers, Journal of Power and Energy Systems 2 (5) (2008) 1198–1208.
[11] H. Karabulut, H.S. Yücesu, A. Koca, Manufacturing and testing of a V-type Stirling engine, Turk. J. Eng. Environ. Sci. 24 (2) (2000) 71–80.
[12] C. Cinar, et al., Beta-type Stirling engine operating at atmospheric pressure, Appl. Energy 81 (4) (2005) 351–357.
[13] A. Sripakagorn, C. Srikam, Design and performance of a moderate temperature difference Stirling engine, Renew. Energy 36 (6) (2011) 1728–1733.
[14] R. Gheith, F. Aloui, S.B. Nasrallah, Determination of adequate regenerator for a Gamma-type Stirling engine, Appl. Energy 139 (2015) 272–280.
[15] X. Lai, et al., Stirling engine powered reverse osmosis for brackish water desalination to utilize moderate temperature heat, Energy 165 (2018) 916–930.
[16] P. Rochelle, L. Grosu, Analytical solutions and optimization of the exo-irreversible Schmidt cycle with imperfect regeneration for the 3 classical types of Stirling engine, Oil & Gas Science and Technology–Revue d'IFP Energies nouvelles 66 (5) (2011) 747–758.
[17] P. Rochelle, LDT Stirling Engine Simulation and Optimization Using Finite Dimension Thermodynamics. Thermo-And GFD Modelling of Stirling Machines, 2005, pp. 358–366.
[18] M.H. Ahmadi, A.H. Mohammadi, S.M. Pourkiaei, Optimisation of the thermodynamic performance of the Stirling engine, Int. J. Ambient Energy 37 (2) (2016) 149–161.
[19] L. Grosu, P. Rochelle, N. Martaj, An engineer–oriented optimisation of Stirling engine cycle with finite–size finite–speed of revolution thermodynamics, Int. J. Exergy 11 (2) (2012) 191–204.
[20] S.M.H.W. Dawi, et al., Gamma stirling engine for a small design of renewable resource model, Indonesian Journal of Electrical Engineering and Computer Science 8 (2) (2017) 350–359.
[21] S. Alfarawi, R. Al-Dadah, S. Mahmoud, Influence of phase angle and dead volume on gamma-type Stirling engine power using CFD simulation, Energy Convers. Manag. 124 (2016) 130–140.
[22] B. Kongtragool, S. Wongwises, Thermodynamic analysis of a Stirling engine including dead volumes of hot space, cold space and regenerator, Renew. Energy 31 (3) (2006) 345–359.
[23] S. Kwankaomeng, B. Silpsakoolsook, P. Savangvong, Investigation on stability and performance of a free-piston stirling engine, Energy Procedia 52 (2014) 598–609.
[24] D. Sarkar, Thermal Power Plant: Design and Operation, Elsevier, 2015.
[25] I. Urieli, D.M. Berchowitz, Stirling Cycle Engine Analysis, A. Hilger, Bristol, UK, 1984.
[26] M. Campos, J. Vargas, J. Ordonez, Thermodynamic optimization of a Stirling engine, Energy 44 (1) (2012) 902–910.
[27] J.R. Senft, Theoretical limits on the performance of Stirling engines, Int. J. Energy Res. 22 (11) (1998) 991–1000.
[28] W.R. Martini, Stirling Engine Design Manual, US Department of Energy, Office of Conservation and Solar Applications, 1978.
[29] J.P. Holman, Heat Transfer-Si Units-Sie, Tata McGraw-Hill Education, 2002.
[30] M. Kuosa, et al., Oscillating flow in a stirling engine heat exchanger, Appl. Therm. Eng. 45 (2012) 15–23.
[31] A. Winkelmann, E.J. Barth, Design, modeling, and experimental validation of a stirling pressurizer with a controlled displacer piston, IEEE ASME Trans. Mechatron. 21 (3) (2015) 1754–1764.
[32] T. Colmant, et al., Quasi steady flow modelling of a small Stirling engine: comparison between calculated and measured instantaneous temperatures, in: Proceedings of the 11 th Int. Stirling Engine Conf., ISEC, 2003.
[33] Y.K. Ahn, J.D. Song, B.-S. Yang, Optimal design of engine mount using an artificial life algorithm, J. Sound Vib. 261 (2) (2003) 309–328.
[34] M. Hooshang, et al., Optimization of Stirling engine design parameters using neural networks, Renew. Energy 74 (2015) 855–866.
[35] G. Walker, An optimization of the principal design parameters of Stirling cycle machines, J. Mech. Eng. Sci. 4 (3) (1962) 226–240.
[36] M.H. Ahmadi, M.A. Ahmadi, M. Mehrpooya, Investigation of the effect of design parameters on power output and thermal efficiency of a Stirling engine by thermodynamic analysis, Int. J. Low Carbon Technol. 11 (2) (2016) 141–156.
[37] R.E. English, W.W. Wachtl, Charts of Thermodynamic Properties of Air and Combustion Products from 300 to 3500 R, National Advisory Committee for Aeronautics, 1950.
[38] C.-H. Cheng, H.-S. Yang, Optimization of geometrical parameters for Stirling engines based on theoretical analysis, Appl. Energy 92 (2012) 395–405.

[39] C. Cinar, H. Karabulut, Manufacturing and testing of a gamma type Stirling engine, Renew. Energy 30 (1) (2005) 57–66.
[40] A.T. Shiferaw, et al., Design of a Stirling Engine for Electricity Generation, 2014.
[41] R.J. Moffat, Describing the uncertainties in experimental results, Exp. Therm. Fluid Sci. 1 (1) (1988) 3–17.
[42] G. Xiao, et al., An approach to combine the second-order and third-order analysis methods for optimization of a Stirling engine, Energy Convers. Manag. 165 (2018) 447–458.
[43] M. Khanjanpour, et al., An investigation of a Ɣ-type MTD Stirling engine prototype, in: UK Association for Computational Mechanics Conference 2019, London, United Kingdom, 2019, 10th - 12th Apr 2019.
[44] C.-H. Cheng, H.-S. Yang, Optimization of rhombic drive mechanism used in beta-type Stirling engine based on dimensionless analysis, Energy 64 (2014) 970–978.
[45] H. Damirchi, et al., Micro combined heat and power to provide heat and electrical power using biomass and Gamma-type Stirling engine, Appl. Therm. Eng. 103 (2016) 1460–1469.
[46] Kwasi-Effah, C., et al., Review of Existing Models for Stirling Engine Performance Prediction and the Paradox Phenomenon of the Classical Schmidt Isothermal Model.
[47] S. Zare, A. Tavakolpour-Saleh, M. Sangdani, Investigating limit cycle in a free piston Stirling engine using describing function technique and genetic algorithm, Energy Convers. Manag. 210 (2020) 112706.
[48] A. Masoumi, A. Tavakolpour-Saleh, Experimental assessment of damping and heat transfer coefficients in an active free piston Stirling engine using genetic algorithm, Energy 195 (2020) 117064.
[49] J. Egas, D.M. Clucas, Stirling engine configuration selection, Energies 11 (3) (2018) 584.
[50] A.J. Organ, The Regenerator and the Stirling Engine, vol. 624, Mechanical Engineering Publications, London, 1997.
[51] M. Yunus, M.S. Alsoufi, A.K. Rathod, Design, manufacture and measurements of beta-type stirling engine with rhombic drive mechanism, Mod. Mech. Eng. 6 (2016) 113, 04.
[52] H.-J. Shih, An analysis model combining gamma-type stirling engine and power converter, Energies 12 (7) (2019) 1322.
[53] S.-W. Kang, et al., Fabrication and test of gamma-type Stirling engine, in: Proceedings of the International Conference on Energy and Sustainable Development: Issues and Strategies (ESD 2010), IEEE, 2010.
[54] M. Chahartaghi, M. Sheykhi, Energy, environmental and economic evaluations of a CCHP system driven by Stirling engine with helium and hydrogen as working gases, Energy 174 (2019) 1251–1266.
[55] R. Gheith, F. Aloui, S.B. Nasrallah, Study of the regenerator constituting material influence on a Gamma type Stirling engine, J. Mech. Sci. Technol. 26 (4) (2012) 1251–1255.
[56] R.R. Hegde, et al., Assessing IP, FP and BP of diesel engine fueled with diesel and water-in-diesel emulsion using different surfactants, Inven. Impact Combust. 4 (2014) 187–191.